Seventh Framework Programme
Theme 9 Space FP7-SPA.2009.1.1.02
Monitoring of climate change issues (extending core service activities)

Grant agreement for: Collaborative Project (generic).
Project acronym: **MONARCH-A**
Project title: **MONitoring and Assessing Regional Climate change in High latitudes and the Arctic**
Grant agreement no. 242446
Start date of project: 01.03.10
Duration: 36 months
Project coordinator: Nansen Environmental and Remote Sensing Center, Bergen, Norway

D1.5.2: Analysis of feedback mechanisms on climate and carbon from reanalysis calculations

Due date of deliverable: 31.05.2013

Actual submission date: 31.05.2013

Organization name of lead contractor for this deliverable: USFD

Project co-funded by the European Commission within the Seventh Framework Programme, Theme 6 Environment		
Dissemination Level		
PU	Public	X
PP	Restricted to other programme participants (including the Commission)	
RE	Restricted to a group specified by the consortium (including the Commission)	
CO	Confidential, only for members of the consortium (including the Commission)	

ISSUE	DATE	CHANGE RECORDS	AUTHOR
1	31/05/2013	Report	S. Quegan

SUMMARY

The land surface at Northern high latitudes is home to a wide range of interacting processes and feedbacks, many of them mediated through two-way land-atmosphere fluxes of energy, water and trace gases. The land surface also has important consequences for the Arctic Ocean as a source of inputs of fresh water and nutrients, but feedbacks from the ocean are indirect, through the atmosphere. The calculations carried out in Theme 1 of MONARCH-A embody these interactions and feedbacks within the framework of a set of state-of-the-art Land Surface Models.

MONARCH-A did not consider the full set of feedbacks in the system because it did not have an atmospheric component, but models were used to explore links and feedbacks between the terrestrial variables, which in several case involved modifying the models. This report summarises these investigations, and makes more explicit feedbacks that are implicit in the calculations.

In particular, we indicate how methodologies that were developed during the project to interface land cover, fire and snow ECVs to models could improve model parameterizations and reduce uncertainties in simulated carbon and water fluxes for northern latitudes.

MONARCH-A CONSORTIUM

Participant no.	Participant organisation name	Short name	Country
1 (Coordinator)	Nansen Environmental and Remote Sensing Center	NERSC	NO
2	The University of Sheffield	USFD	UK
3	Universität Hamburg	UHAM	NO
4	Centre National de la Recherche Scientifique	CNRS	FR
5	Scientific foundation Nansen International Environmental and Remote Sensing Center	NIERSC	RU
6	Universitetet i Bergen	UiB	NO
7	Danmarks Tekniske Universitet	DTU	DK
8	Institut Francais de Recherche pour l'Exploitation de la Mer	IFREMER	FR

Table of Contents

List of figures

List of Tables

1 Introduction

The land surface at Northern high latitudes is home to a wide range of interacting processes and feedbacks, many of them mediated through two-way land-atmosphere fluxes of energy, water and trace gases. The land surface also has important consequences for the Arctic Ocean as a source of inputs of fresh water and nutrients, but feedbacks from the ocean are indirect, through the atmosphere. The complexity and range of the land-atmosphere interactions is indicated by Fig. 1.

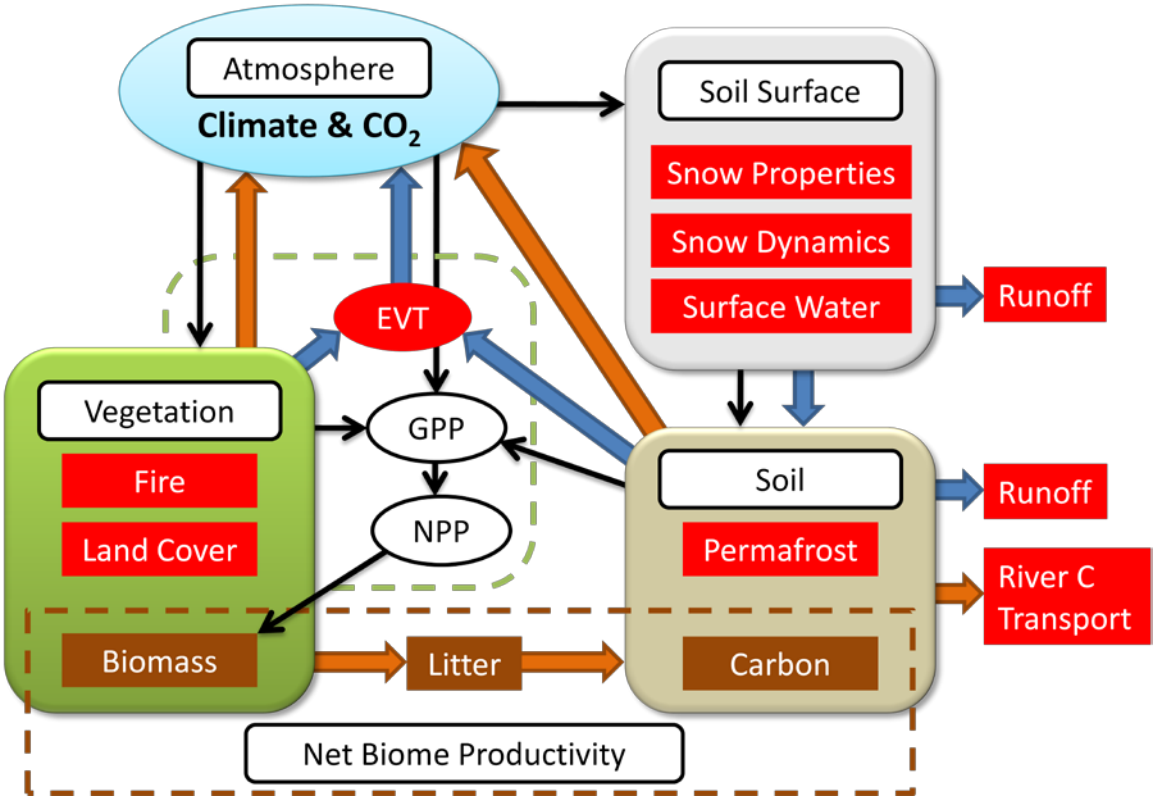

Figure 1: System diagram illustrating how models integrate processes and variables to represent the carbon and water cycles. Red boxes indicate ECVs considered in MONARCH-A (though no calculations of river C transport were carried out and biomass is also an ECV), brown boxes indicate the terrestrial carbon pools, orange arrows indicate fluxes of carbon from the terrestrial carbon pools, blue arrows indicate fluxes of water, and black arrows are used to indicate processes and subsidiary fluxes.

The overall carbon balance is indicated in this diagram by the Net Biome Productivity, which is the net flow of carbon into the land surface when all processes have been considered, and can be written in two forms, the **mass balance or allocation equation**:

$$\Delta C = \Delta B_A + \Delta B_B + \Delta L + \Delta S \qquad \text{(Eq. 1)}$$

and the **process equation**:

$$\Delta C = GPP - R_P - R_H - D = NPP - R_H - D - T_R \qquad \text{(Eq. 2)}$$

Here Δ indicates a change and the other symbols are defined as follows:

C carbon sequestered by vegetation and soil; negative values imply loss to the atmosphere

B biomass (*A*: above and *B*: below ground),

L litter,

S soil carbon,

GPP Gross Primary Production (photosynthesis),

NPP Net Primary Production: $NPP = GPP - R_P$,

R respiration (*P*: plant and *H*: heterotrophic),

D carbon loss by disturbance (mainly fire)

T_R soil carbon going into rivers and lost by transport.

The corresponding net water balance is given by

$$P - EVT - R - \Delta M_S - S_s - S_C - T - T_s = 0, \quad \text{(Eq. 3)}$$

where the terms are defined as follows:

P precipitation (snowfall),

EVT evapotranspiration

R runoff

M_S soil moisture

S_S snowpack sublimation,

S_C canopy sublimation,

T wind transport or blowing snow,

T_S sublimation of blowing snow.

The terms in these equations can be treated as instantaneous and hence as rates, or as integrated over a period of time, in which case they correspond to quantities of carbon (eqs. [1] & [2]) or of water (eq. [3]). The spatial unit of these equations can also be the model grid-cell or an integrated value over a region, such as a catchment.

The model calculations carried out in Theme 1 of MONARCH-A have been based on these equations as they are embodied in a range of state-of-the-art Land Surface Models. Since these models integrate all processes in a unified framework, feedbacks are implicit in the calculations, but in what

follows we describe work performed to make some of them more explicit (and indeed to include some feedbacks not found in the original models).

Note that MONARCH-A did not consider the full set of feedbacks in the system because it did not have an atmospheric component. For example, there is a complex interplay between snow cover, land cover and albedo as regards the energy balance of the atmosphere. Similarly, we did not consider the feedbacks between a warming climate and greenhouse gas (GHG) emissions, where we would expect warming to drive increased soil respiration, hence greater atmospheric loading by GHGs, but offset by increased vegetation growth due to both higher temperatures and carbon fertilization. Instead we used models to explore links between the terrestrial variables, in several case modifying models to do this. In this report we summarise these investigations.

In particular, during realization of deliverable D1.5.1: "*Software modules interfacing variables derived in WP 1.1-1.4 to models*", methodologies were developed that interface Essential Climate Variables (ECVs) with dynamic vegetation models. In the present deliverable, we show how these methodologies can improve model parameterizations and reduce uncertainties by forcing and assimilating ECVs into models and performing a reanalysis on simulated carbon and water fluxes in the northern latitudes.

2 Essential Climate Variables

2.1 Land Cover

A complete methodology for driving dynamic vegetation models with land cover data was delivered in MONARCH-A as a requisite for deliverable D1.4.1: '*Analysis of available land cover and fire products and recommendations for use in climate models'* and D1.5.1*: 'Software modules interfacing variables derived for W.P 1.1-1.4 to models'*. Therefore in this section we will briefly describe the key points and results; more information can be found in the deliverables mentioned above.

A source of uncertainty in model estimates of Net Biome Production (NBP), fire emissions and water fluxes is land cover. Most land surface models require land cover maps as inputs in order to determine the characteristics of the overlying vegetation and apply the appropriate physical processes. These maps usually originate from classification of Earth Observation data sets, of which four of the most widely used are: GlobCover [*Arino et al.*, 2008], GLC2000 [*Bartholome and Belward*, 2005], MODIS LC [*Friedl et al.*, 2010] and the Vegetation Continuous Field (VCF) product derived from MODIS [*Hansen et al.*, 2003]. During realization of the deliverable D1.4.2: *Land cover maps transformed into forms suitable for climate modeling* it was established that they exhibit great differences (Fig. 2 (top)). To evaluate the effects of these differences and the uncertainties they impose on the resulting carbon fluxes of a land surface model we used these 4 land cover datasets to drive the Sheffield Dynamic Global Vegetation Model (SDGVM) [*Woodward et al.*, 1995]. The resulting average fluxes making up the carbon balance of the pan-boreal region over the period 1981-2006 are presented in Fig. 2 (bottom). Despite large differences in the proportions in the three generic land cover types (tree, herbaceous and bare cover) in the land cover maps (Fig. 2 (top)), Net Primary Productivity (NPP) and Heterotrophic Respiration (R_h) show differences of only a few per cent between the various land covers. Larger differences occur in Net Ecosystem Production (NEP) and fire emissions. Since SDGVM treats only above-ground biomass as fuel, fire emissions are roughly linearly proportional to tree cover, so the largest difference is between GLC2000 (40% tree cover) and MODIS VCF (25% tree cover), with the latter giving almost 50% lower emissions. NBP for pan-boreal latitudes was found to be well-approximated (adjusted R^2 = 0.69) by a linear function of tree and grass cover given by:

$$NBP = 6.82(\pm 1.96) \times (\text{Tree Cover}) + 2.98(\pm 1.31) \times (\text{Grass Cover}) \quad \text{(Eq. 4)}$$

with NBP in units of 10^{14} gC yr^{-1} and cover expressed as a fraction between 0 and 1. This leads to differences of 20% between the lowest carbon uptake (GlobCover) and highest (GLC2000); GlobCover has the highest fraction of bare ground, while GLC2000 has the least bare ground and the highest amount of tree cover.

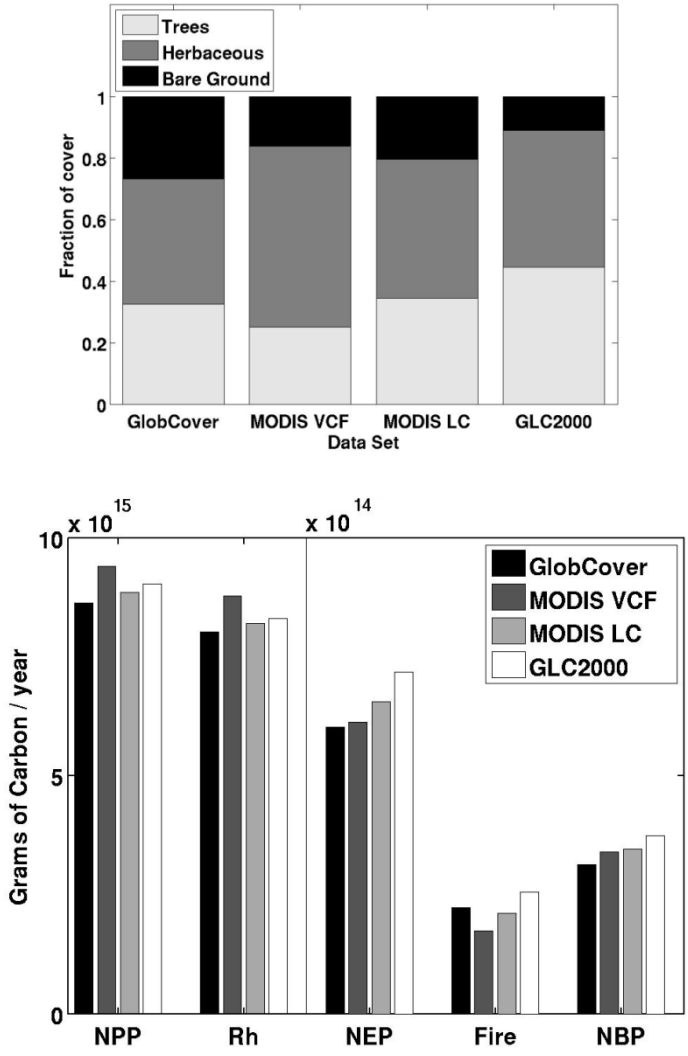

Figure 2: (top) Pan-boreal fractions of three generic cover types (trees, herbaceous cover and bare ground) derived from the four land cover maps. (bottom) Average values of pan-boreal NPP, R_h, NEP, fire emissions and NBP calculated by SDGVM over the period 1981-2006 when driven with GlobCover, MODIS VCF, MODIS LC and GLC2000.

2.2 Burned Area

As with land cover, assimilating burned area data in dynamic vegetation models was carried out using the methods described in deliverable D1.5.1*: 'Software modules interfacing variables derived*

for W.P 1.1-1.4 to models'. Here we show the main results, which are presented in greater detail in Kantzas et al. [2013a](under rev).

Comparison of model outputs of burned area with EO data (the Global Fire Emissions Database-Burned Area, [*van der Werf et al.*, 2010]) collected for deliverable D1.4.1: *'Analysis of available land cover & fire products*' revealed that modeled burned area had significantly less inter-annual variability (IAV) than the observations. The effects were investigated by modifying SDGVM so as to force the calculated IAV of burned area to be consistent with that observed in GFED-BA (Fig. 3).

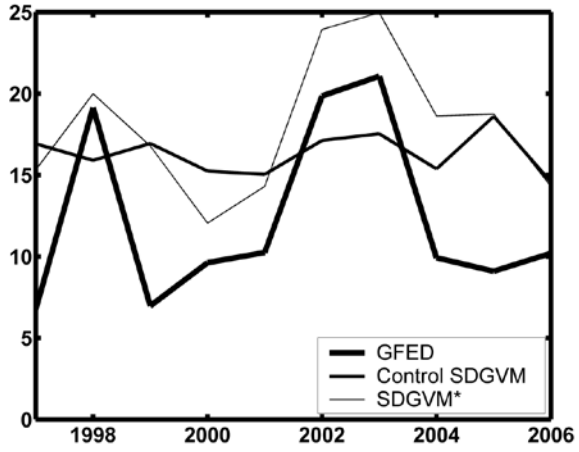

Figure 3: Burned area (in Mha) from GFED-BA, SDGVM and the SDGVM with the adjusted burnt area (denoted as SDGVM) for the pan-boreal region for 1997-2006.*

Shown in Fig. 4 are time series (1960-2006) of the de-trended NBP (lower plot) and fire emissions (upper plot) calculated by SDGVM and SDGVM*. As expected, the inter-annual variability of the fire emissions increases significantly as a result of the increased variability in burnt area. However, the inter-annual variability of NBP is not significantly affected, and there is little correlation between NBP and the size of the emissions. Although the variance of the NBP in the adjusted run increased by 15.0%, only 22% of the adjusted NBP variance can be attributed to the variance of the adjusted fire emissions; this is insufficient to affect the sign of the NBP and turn a carbon dioxide sink year into a source and vice versa. Although the IAV of the burnt area now corresponds much more closely to that of the observations, the mean behavior and trends of burnt area, emissions and NBP are unaffected. In other words, for the pan-boreal region, fire emissions do not appear to be the major driver of the observed variability of land-atmosphere carbon exchange. This is consistent with the finding of *Prentice et al.* [2011] that (at global scale) during 1997-2005, the CO_2 fluxes produced by GFED would have contributed only a third of the variability in total CO_2 flux inferred from atmospheric inversion, despite earlier studies postulating that biomass burning contributes greatly to land-atmosphere carbon flux anomalies [*Nevison et al.*, 2008; *Patra et al.*, 2005]. In the case

presented here, fire emissions contribute around 22% of the variability of the CO_2 flux. More details can be found in deliverable D1.4.3: *'Integrated Fire Products for Carbon & Climate Modeling*'.

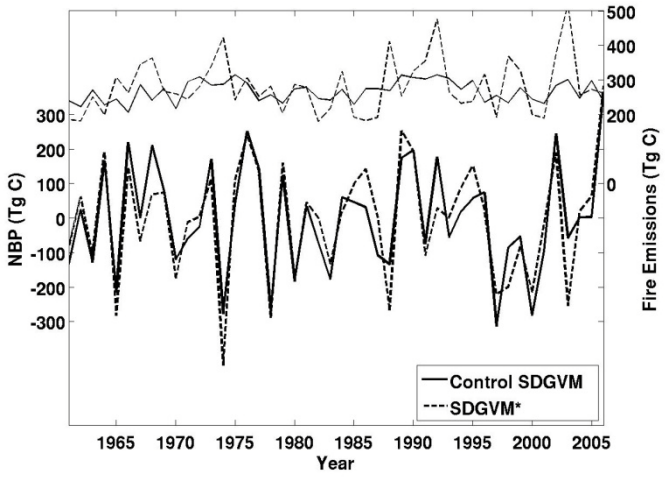

Figure 4: Time series (1960-2006) of the de-trended NBP (solid lines, left y-axis) and fire emissions (dashed lines, right y-axis) for SDGVM and its modified version, SDGVM.*

2.3 Snow Water Equivalent

2.3.1 Optimization

The field data chosen to be assimilated in a dynamic vegetation model was the FSU Hydrological Snow Surveys dataset [*Krenke*, 2004], which consists of snow transect measurements carried out from 1966-1996 in the proximity of 1,345 World Meteorological Organisation (WMO) stations spread throughout the FSU (Fig. 5). The number of stations in the data set reduced from 1,345 in 1990 to about 200 in 1991, the majority of which are located in the European sector of the FSU, with very little coverage over northern Siberia. Each station exhibits different and varying sampling frequency, but measurements of snow water equivalent (SWE), snow depth and snow density are usually taken every 5 or 10 days. A model-independent optimization method was sought which would use the field available records of SWE to improve model snow parameterization and consequently simulations. A fast model was desirable as any multi-dimensional optimization routine would likely require hundreds of computations of an error function. For this study the SDGVM was used, as it is the fastest model available in our model suite due to its relatively large time step (daily as opposed to hourly) and simple process descriptions. For the observational data, monthly averages were produced from the transect data. The optimization process consists of finding the minimum of an error function that describes the difference between model and observation. The error function was taken to be the average absolute monthly difference in snow months between observation and model, averaged over all sites, where a snow month is defined as any month having a positive value

of SWE, either observed or modeled. For the optimization, a modified version of the 'Downhill Simplex Method in Multi-dimensions' [*Press et al.*, 1992] was employed. This algorithm was modified to allow sensible constraints to be applied to the physical optimization parameters.

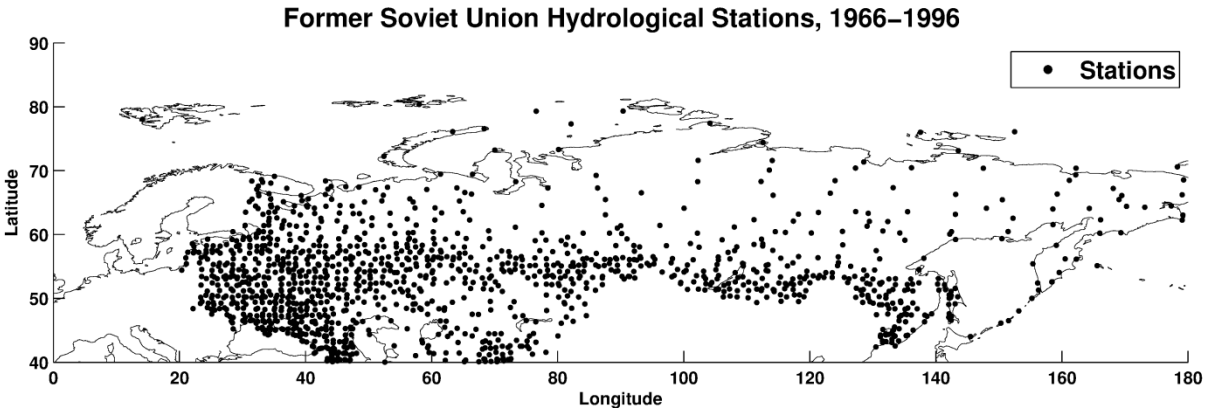

Figure 5: Location of hydrological stations considered in this study; note the scarcity over northern Siberia.

The optimization was carried out over four parameters which were expected to play a major role in the timings and dynamics of the snowpack:

1. The average daily temperature for which snow occurs, which determines the start date of the snowpack and is set to 0 ^{o}C in the unmodified SDGVM;
2. The average daily temperature at which snow melts, which affects the end date of the snowpack and is also set to 0 ^{o}C;
3. The rate at which snow melts, which affects the end date of the snowpack and is proportional to temperature;
4. The sublimation rate, which affects the overall size of the snowpack and is proportional to potential evapotranspiration.

The system is biased towards Western Eurasia because of the high concentration of observational sites there (Fig. 5). This has been mitigated to some extent by restricting the sites used for the optimization to one per 2^{o} grid-cell of latitude and longitude, and using the site with most observations when multiple sites occur in such a grid-cell.

After the optimization process, the average absolute error in monthly SWE between SDGVM and transect measurements reduced from 33.9 mm to 28.3 mm, largely because of the reduction of SWE in the Western sector, where the temporal correlation also improved (Fig. 6, SDGVM-Opt). The

optimization leads to particularly large changes in the temperature limit for snow start and the sublimation rate (Table 1).

Parameter	SDGVM	SDGVM-Opt
Snow start temperature limit	0 °C	-4.38 °C
Snow melt temperature limit	0 °C	0.61 °C
Snow melt rate factor	1	0.31
Sublimation rate factor	1	3.79

Table 1: Original and optimized parameters in the SDGVM model: snow start temperature limit (° C), snow melt temperature limit (° C), snow melt rate factor and sublimation rate factor. The last two terms are dimensionless and refer to the factor by which the estimated melt rate and sublimation are multiplied compared to the unmodified SDGVM.

The reduction in the snow start temperature limit leads to a shorter snow season, causing less snow to be produced over the year for all sites. The nearly factor 4 increase in the sublimation rate also reduces the SWE because of increased loss to the atmosphere; this indicates that sublimation is underestimated in SDGVM, in agreement with Kantzas et al. [2013b](under rev.), Section 4.4. Both these changes reduce the overestimation of SWE by the model and improve its description of snow dynamics in the west.

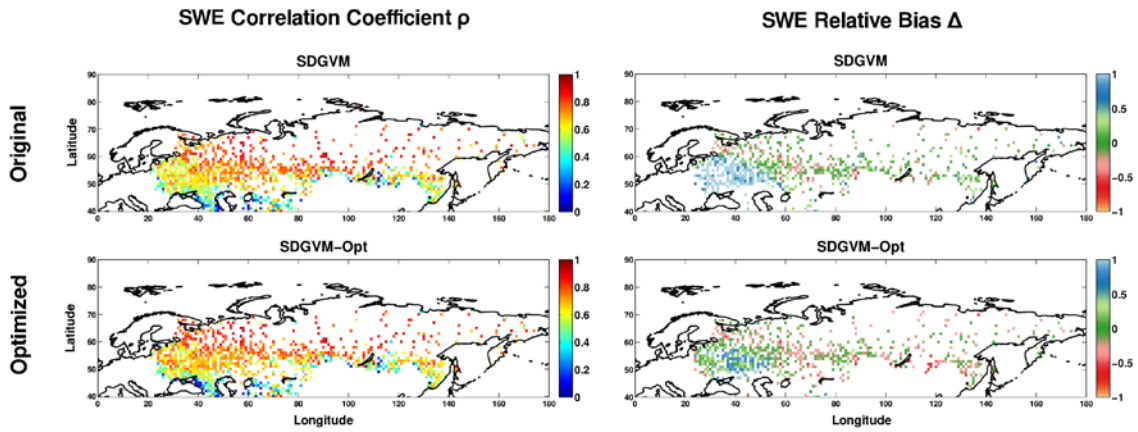

Figure 6: (left) Correlation coefficient of monthly SWE, ρ, between the transect records and calculations for the original and optimized form of SDGVM for 1966-1996 across the FSU. (right) Relative bias Δ, a measure of over/under-estimation, between the transect records and SDGVM for grid-cells with ρ ≥ 0.6.

2.3.2 Driving model with data

The 30-year time-span and 5- to 10-day temporal spacing of the FSU field records provide sufficient data on snow variables, such as depth and density, to force the heat diffusion formulation of the LPJ-

WM model [*Wania et al.*, 2009]. Furthermore, since this model treats snow density as constant except in the last quarter of the snow season, comparison of model calculations with and without imposing observed values of snow density offers insight into the feedbacks from a simplified evolution of snow density.

Differences between modeled and field values of snow depth and density for three field stations are shown in Fig. 7, together with values of soil temperature at 25 cm depth estimated by the model in its unmodified form, and when driven by observed snow depth alone (LPJ-WM S)and by both depth and density (LPJ-WM SD). As expected, where LPJ-WM overestimates snow depth, modeled soil temperatures are lower in winter when the model is forced by observed snow depth. This is illustrated by Fig. 7 (top) for the Njuja station in eastern Siberia in a region of continuous permafrost. Winter soil temperatures dropped significantly, with an average decrease of 6°C at 25 cm depth during January for the period 1966-1996. However, there was little difference in soil temperature for the upper soil layers during the late spring and summer months. As a consequence, the integrated annual heterotrophic respiration decreased by approximately 7.4%, but the summer thaw depth was unaffected. Note that, for the 9 stations examined, the biggest difference in snow depth between LPJ-WM and field data was at Njuja, and so the largest differences in heterotrophic respiration were observed here.

The Tevriz station is located in central Siberia and here LPJ-WM places the permafrost boundary at a depth just below 25 cm (Fig. 7, middle). Here there is less consistency between modeled and observed snow depth than at Njuja, with good agreement in some years but overestimates in others. The soil response is also less consistent: significant overestimates of snow depth do not always yield reduced winter temperatures (for example, in 1983 or 1984). In fact, for those particular years, even though field data had indeed less snow than the model, they also showed an earlier start to the snow season which compensated for the reduced snow depth later on and prevented a lower soil temperature. Although temperature differences up to 5°C are observed for January in 1980 and 1981 for the Tevriz station, the summer temperature shows only a small decrease, so again the thaw depth is unaffected while heterotrophic respiration reduces by 7.3%.

At Olekminsk station in Eastern Siberia, the magnitude and timing of snow depth are very similar in LPJ-WM and field data (Fig. 7, bottom) so forcing the model with field data has little effect on the simulated soil temperatures, and causes integrated annual heterotrophic respiration to reduce by only 1.3%. Additionally, as for the other 2 stations, it was found that forcing the model with snow depth and snow density made little to no difference to soil temperatures than when forcing it with

snow depth alone. It was therefore demonstrated that even though simulations of soil temperature and consequently soil carbon decomposition in LPJ-WM are sensitive to inaccuracies of both snow magnitude and timing, soil temperature simulations are robust towards snow density and the simplified approach of LPJ-WM is deemed adequate.

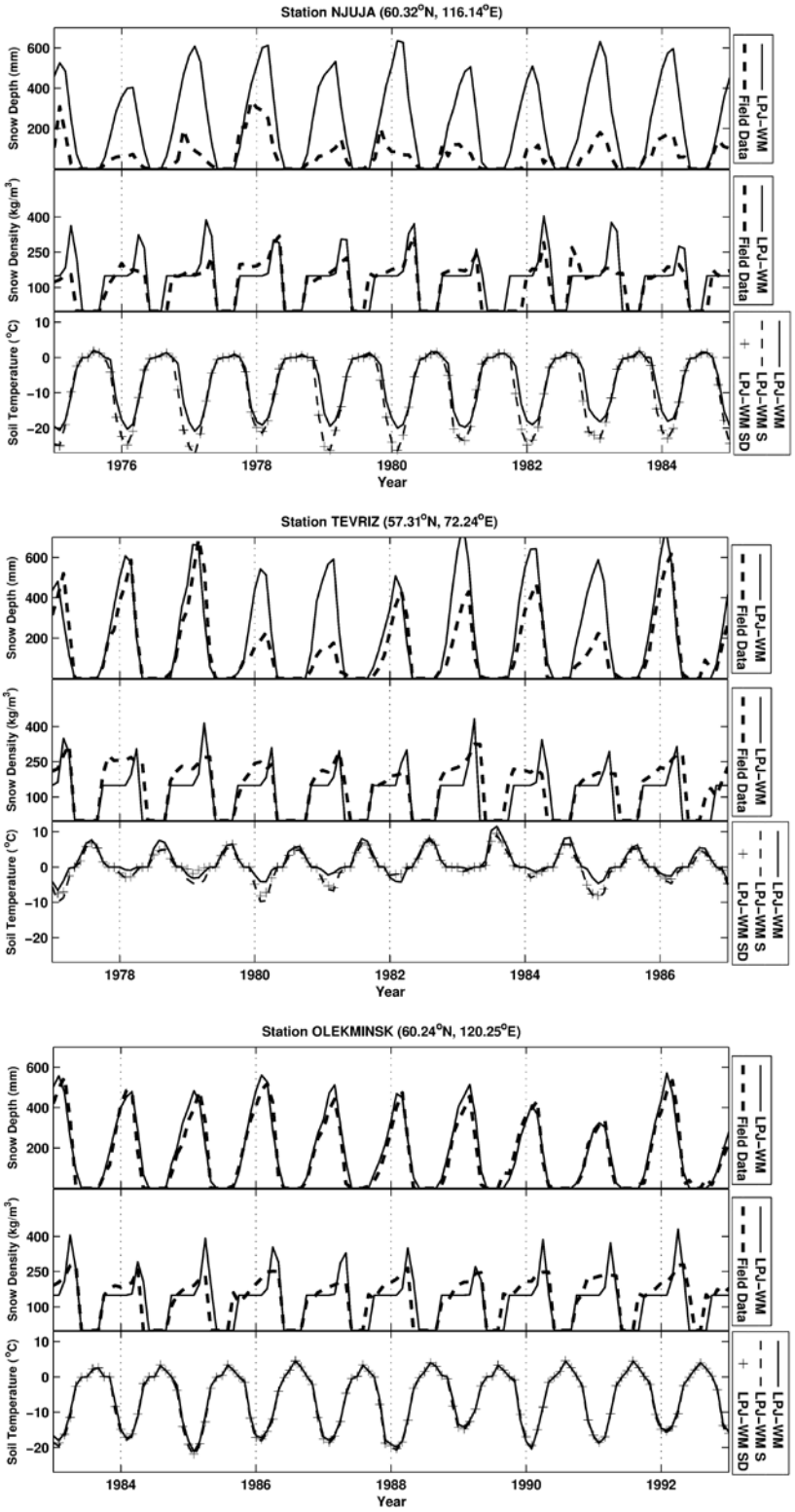

Figure 7: Snow depth (mm) and snow density (kg/m^3) from LPJ-WM and field records for 3 WMO stations located in Eastern and Central Siberia. The bottom subplot in each figure shows the monthly soil temperature (°C) at a depth of 25 cm produced by LPJ-WM, along with the corresponding temperature when the model is driven by snow depth alone (LPJ-WM S) and both snow depth and density (LPJ-WM SD) using values taken from the field records.

3 Conclusions

State-of-the-art Land Surface Models have been interfaced with ECV datasets in order both to explore the uncertainty in their calculations and to improve the accuracy with which they represent high latitude processes that are crucial in estimating carbon and water balances. By their nature, models contain process interactions and feedbacks that are usually implicit. Modifying the models to provide a reanalysis driven by knowledge of key ECVs has helped to make these dependencies explicit. Other work carried put in the project has also indicated fundamental connections and feedbacks between processes, such as land cover, fire, biomass and permafrost, which have a bearing on both the carbon and water balances. This analysis would be even more powerful if carried out within the framework of a coupled land-atmosphere model, since several crucial feedbacks involving energy and trace gas fluxes could not be considered without an atmospheric component in MONARCH-A.

4 References

Arino, O., P. Bicheron, F. Achard, J. Latham, R. Witt, and J. L. Weber (2008), GLOBCOVER: The most detailed portrait of Earth, *Esa Bull-Eur Space*(136), 24-31.

Bartholome, E., and A. S. Belward (2005), GLC2000: a new approach to global land cover mapping from Earth observation data, *Int J Remote Sens*, *26*(9), 1959-1977, doi: 10.1080/01431160412331291297.

Friedl, M. A., D. Sulla-Menashe, B. Tan, A. Schneider, N. Ramankutty, A. Sibley, and X. M. Huang (2010), MODIS Collection 5 global land cover: Algorithm refinements and characterization of new datasets, *Remote Sens Environ*, *114*(1), 168-182, doi: 10.1016/j.rse.2009.08.016.

Hansen, M. C., R. S. DeFries, J. R. G. Townshend, M. Carroll, C. Dimiceli, and R. A. Sohlberg (2003), Global Percent Tree Cover at a Spatial Resolution of 500 Meters: First Results of the MODIS Vegetation Continuous Fields Algorithm, *Earth Interact*, *7*.

Kantzas, E., M. Lomas, and S. Quegan (2013a), Fire at high latitudes: data-model comparisons and their consequences, *Global Biogeochem Cy*.

Kantzas, E., M. Lomas, S. Quegan, and E. Zakharova (2013b), Evaluation of the snow regime in dynamic vegetation land surface models using field measurements, *The Cryosphere Discuss.*, *7*(3), 2333-2372, doi: 10.5194/tcd-7-2333-2013.

Krenke, A. (2004), Former Soviet Union hydrological snow surveys, edited, NSIDC, Boulder,CO.

Nevison, C. D., N. M. Mahowald, S. C. Doney, I. D. Lima, G. R. Van der Werf, J. T. Randerson, D. F. Baker, P. Kasibhatla, and G. A. McKinley (2008), Contribution of ocean, fossil fuel, land biosphere, and biomass burning carbon fluxes to seasonal and interannual variability in atmospheric CO(2), *J Geophys Res-Biogeo*, *113*(G1), doi: 10.1029/2007jg000408.

Patra, P. K., M. Ishizawa, S. Maksyutov, T. Nakazawa, and G. Inoue (2005), Role of biomass burning and climate anomalies for land-atmosphere carbon fluxes based on inverse modeling of atmospheric CO2, *Global Biogeochem Cy*, *19*(3), doi: 10.1029/2004gb002258.

Prentice, I. C., D. I. Kelley, P. N. Foster, P. Friedlingstein, S. P. Harrison, and P. J. Bartlein (2011), Modeling fire and the terrestrial carbon balance, *Global Biogeochem Cy*, *25*, doi: 10.1029/2010gb003906.

Press, W. H., S. A. Teukolsky, W. T. Vetterling, and B. P. Flannery (1992), *Numerical Recipes in Fortran: The Art of Scientific Computing*, Cambridge University Press, Cambridge.

van der Werf, G. R., J. T. Randerson, L. Giglio, G. J. Collatz, M. Mu, P. S. Kasibhatla, D. C. Morton, R. S. DeFries, Y. Jin, and T. T. van Leeuwen (2010), Global fire emissions and the contribution of deforestation, savanna, forest, agricultural, and peat fires (1997-2009), *Atmos Chem Phys*, *10*(23), 11707-11735, doi: 10.5194/acp-10-11707-2010.

Wania, R., I. Ross, and I. C. Prentice (2009), Integrating peatlands and permafrost into a dynamic global vegetation model: 1. Evaluation and sensitivity of physical land surface processes, *Global Biogeochem Cy*, *23*, doi: 10.1029/2008gb003412.

Woodward, F. I., T. M. Smith, and W. R. Emanuel (1995), A Global Land Primary Productivity and Phytogeography Model, *Global Biogeochem Cy*, *9*(4), 471-490.

END OF DOCUMENT